Ore Geology Reviews 87 (2017) 16–24

Contents lists available at ScienceDirect

Ore Geology Reviews

journal homepage: www.elsevier.com/locate/oregeorev

Paleomagnetic study of ferromanganese crusts recovered from the northwest Pacific — Testing the applicability of the magnetostratigraphic method to estimate growth rate

Atsushi Noguchi [a,b], Yuhji Yamamoto [a,*], Keisuke Nishi [a], Akira Usui [a], Hirokuni Oda [b]

[a] Kochi University, B200 Monobe, Nankoku, Kochi 783-8502, Japan
[b] Research Institute of Geology and Geoinformation, Geological Survey of Japan, AIST, Central 7, 1-1-1 Higashi, Tsukuba 305-8567, Japan

ARTICLE INFO

Article history:
Received 9 April 2016
Received in revised form 19 July 2016
Accepted 23 July 2016
Available online 27 July 2016

Keywords:
Ferromanganese crusts
Northwest Pacific
Magnetostratigraphy
Growth rates

ABSTRACT

Previous studies have shown that ferromanganese crusts in the Pacific Ocean commonly record paleomagnetic reversals and that the reversal patterns can be used to estimate growth rates. In order to investigate the applicability of the magnetostratigraphic method, we conducted paleomagnetic measurements of crust samples recovered from five locations in the northwest Pacific. A series of thin slices, with thicknesses of 0.5–1.0 mm, was prepared for each sample, and a paleomagnetic polarity was determined for each slice. In all five samples, we found a consistent reversal pattern of N1–R1–N2–R2–N3 from the surface to the inner part of the crust. In three samples, another polarity interval (R3) was recognized below the N3 section of the crust. These data suggest that ferromanganese crusts in the northwest Pacific recorded paleomagnetic reversals and that reversal patterns can be used for ocean-scale correlations. The magnetostratigraphic method suggests constant growth rates of 1.49, 2.54, 3.56 and 3.67 mm/Ma for four samples, three of which are consistent with those estimated using $^{10}Be/^{9}Be$ dating at the 2σ (standard deviation) level.

1. Introduction

Ferromanganese crusts, one of the important marine mineral resources, typically grow on seamounts and their abundance could be estimated by geophysical investigation by multi-channel seismic survey in combination with rock sampling (e.g. Lee et al., 2009). Construction of their reliable age models and hence growth rate estimates are important in understanding the abundance of the crusts. Ferromanganese crusts have been demonstrated to record paleomagnetic reversals. Chan et al. (1985) found six reversals in 13 thin (~1 mm), sequential slices cut from a dredged sample taken from the north Pacific (30°N, 140°W) from the water depth of 3840 m. Linkova and Ivanov (1993) observed six reversals in a series of 10 thin slices (~2–4 mm) cut from a sample taken from the Yuryaku seamount in the central Pacific (32°N, 172°E). Unfortunately, as the most surficial layers of the samples were not characterized by normal polarity (which should be expected for the last 0.78 million years), these studies were not successful in correlating the reversals with the geomagnetic polarity time scale (GPTS). Joshima and Usui (1998) studied three dredged samples recovered from the Nishi–Shichito Ridge (31–32°N, 138–139°E), estimating their growth rates as 14–17 mm/Ma based on 7–10 reversals found in 19–29 thin sequential slices. However, the thickness of the slices (2 mm) seemed to be too large to resolve multiple paleomagnetic polarity records into individual slices, and as a result gave an inaccurate magnetostratigraphy. Oda et al. (2011) successfully constructed a submillimeter scale magnetostratigraphy for one of the Nishi–Shichito Ridge samples using a scanning superconducting quantum interference device (SQUID) microscope. They provided a high-fidelity age model giving an updated growth rate of 5.1 ± 0.2 mm/Ma, which is consistent with the rate of 6.0 ± 0.2 mm/Ma obtained with the $^{10}Be/^{9}Be$ dating method.

The above-mentioned studies have shown that ferromanganese crusts in the Pacific commonly record paleomagnetic reversals and that reversal patterns recorded in the crusts can be used to estimate growth rates. To date, scanning SQUID microscopy on the crust sample from the Nishi–Shichito Ridge by Oda et al. (2011) has been the only successful case for estimating the growth rate based on its magnetostratigraphy. Scanning SQUID microscopy for geological samples is in an early stage of development and not a common method in paleomagnetism and rock magnetism. In this study, we used an ordinary SQUID magnetometer to investigate the applicability of the 'magnetostratigraphic' method. Thin slices were carefully prepared from crust samples recovered from five locations in the northwest Pacific (Ryukyu trench, Ryusei seamount, Hanzawa seamount, Takuyo-Daigo seamount and Nosappu fracture zone), and they were subjected to

* Corresponding author.
E-mail address: y.yamamoto@kochi-u.ac.jp (Y. Yamamoto).

http://dx.doi.org/10.1016/j.oregeorev.2016.07.018
0169-1368/

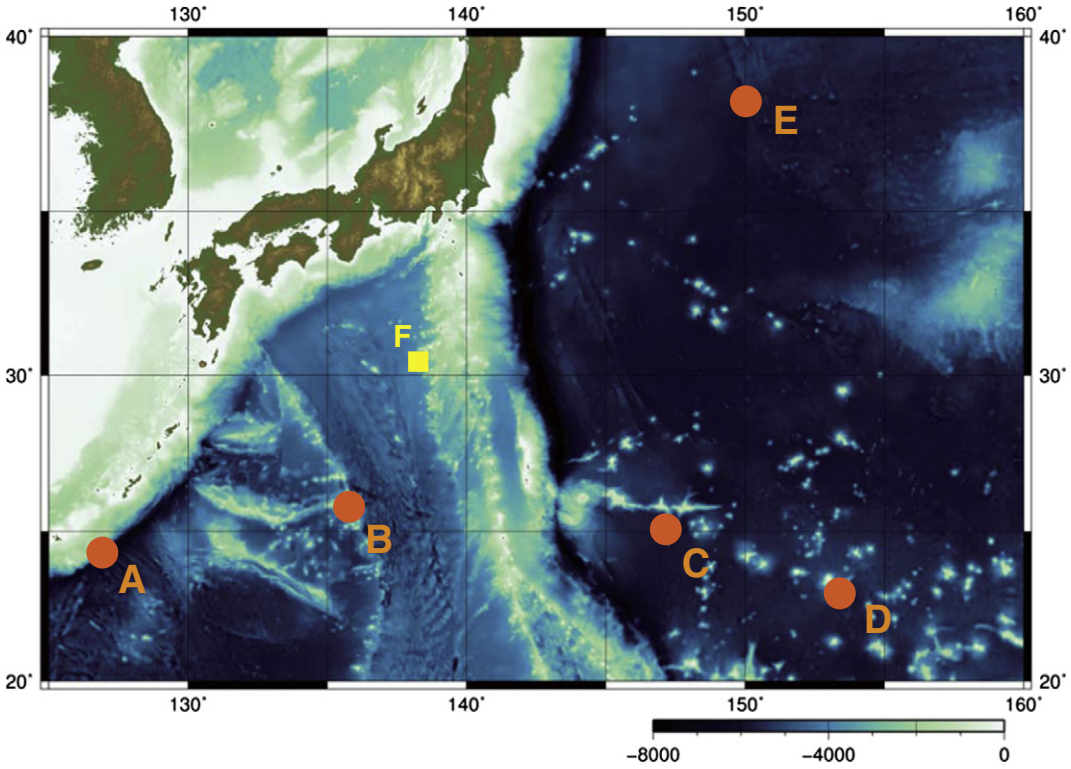

Fig. 1. Location of the sampling sites. (A) Ryukyu trench, (B) Ryusei seamount, (C) Hanzawa seamount, (D) Takuyo-Daigo seamount, and (E) Nosappu fracture zone. (F) Location where sample D96-m4 was taken for the study of Oda et al. (2011).

paleomagnetic measurements. We report and discuss the paleomagnetic measurement results, and estimate a growth rate for each sample based on a magnetic reversal pattern deduced from the results.

2. Material and methods

2.1. Samples

Samples of ferromanganese crusts used in this study were recovered from five locations in the northwest Pacific: Ryukyu trench (24°18.50′N, 127°36.20′E, water depth 6462 m); Ryusei (25°32.37′N, 135°34.33′E, 1529 m), Hanzawa (25°42.58′N, 146°44.90′E, 4362 m) and Takuyo-Daigo (22°41.04′N, 153°14.63′E, 2239 m) seamounts; and Nosappu fracture zone (38°14.27′N, 150°8.27′E, 5961 m) (Fig. 1). The samples were taken with a remotely operated vehicle (ROV) (except for a dredged sample at Nosappu fracture zone) during the cruise KR06-03 for characterization of ferromanganese deposits organized by the Japan Agency for Marine–Earth Science and Technology (JAMSTEC) onboard of R/V Kairei. The advantage of bottom sampling with a ROV is that oceanographic and geochemical parameters are measured on site just above the ferromanganese crusts, and that configurations and occurrences of ferromanganese deposits are observed in detail. A piece of crust can be usually removed from an outcrop with a rotary blade. This method allows selecting only the hydrogenetic crusts firmly attached to rock outcrops, which are also directly overlain by bottom waters without any sediment cover. The approximate gradient of a crust's surface was measured during the operation of the ROV, and was up to 20°. The declinations were not measured during these ROV dives.

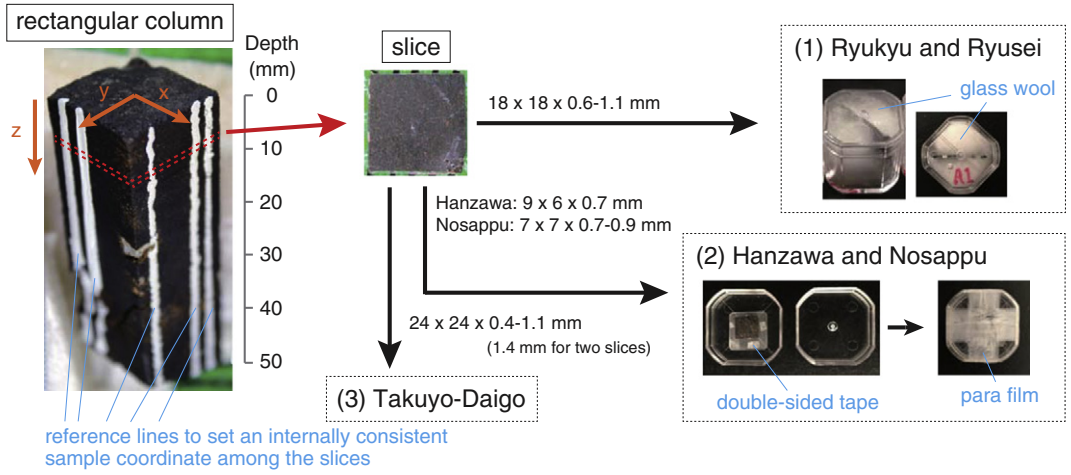

Fig. 2. Sample preparation procedure.

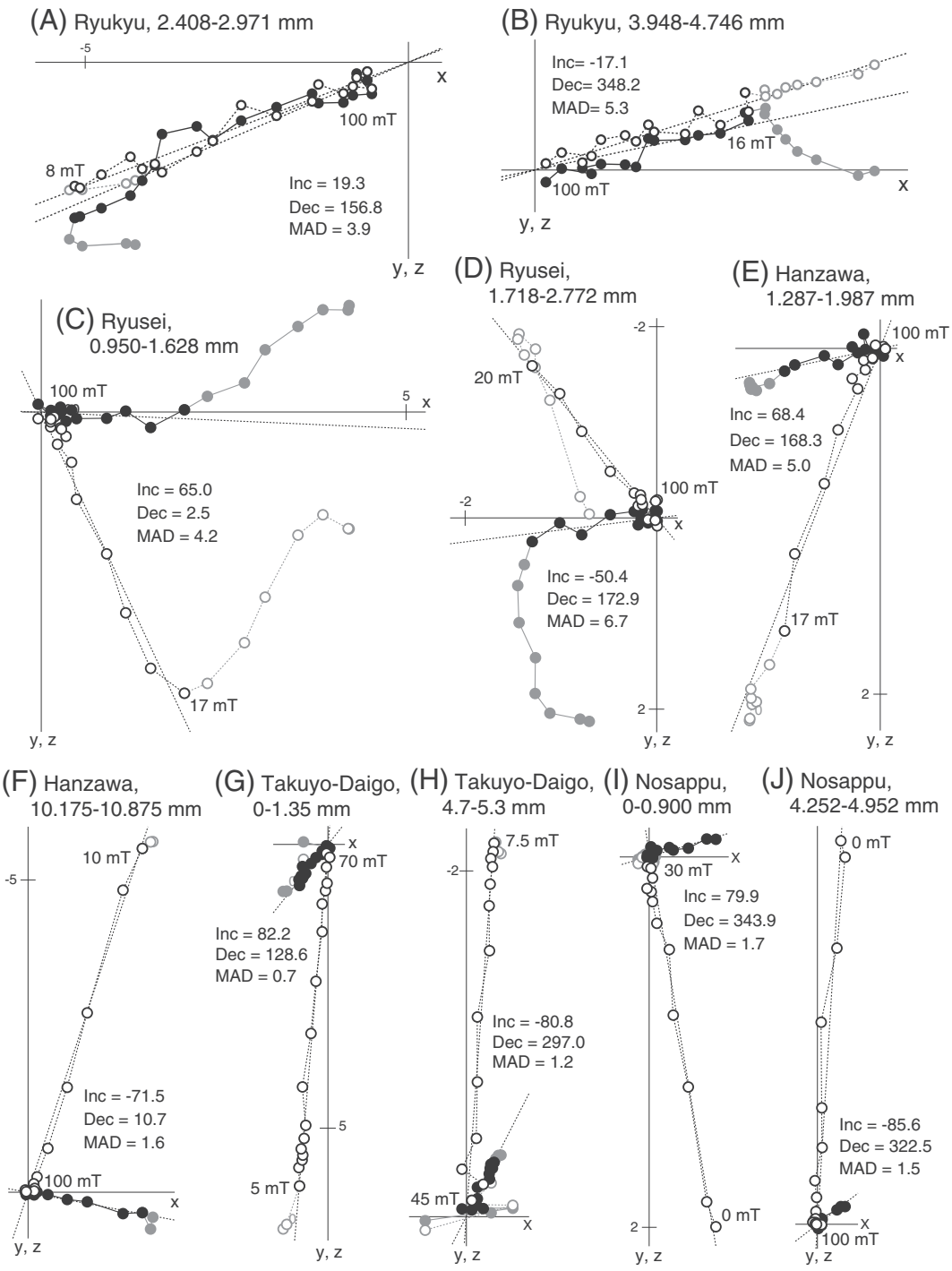

Fig. 3. Representative vector demagnetization diagrams for the slices from the five samples. Ryukyu, depths at 2.408–2.971 mm (A, normal polarity) and 3.948–4.746 mm (B, reversed polarity); Ryusei, depths at 0.950–1.628 mm (C, normal) and 1.718–2.772 mm (D, reversed); Hanzawa, depths at 1.287–1.987 mm (E, normal) and 10.175–10.875 mm (F, reversed); Takuyo-Daigo, depths at 0–1.35 mm (G, normal) and 4.7–5.3 mm (H, reversed); Nosappu, depths at 0–0.900 mm (I, normal) and 4.252–4.952 mm (J, reversed).

Each sample is composed of two parts, a ferromanganese crust, with thickness of about 45–100 mm, and the underlying basalt. The crust has a wavy layered structure parallel to the sample surface with a wavelength of ~6–24 mm. The crust's geochemical and mineral contents, growth structures, and chronology were determined. Results of these analyses are reported by Usui et al. (2017) and Nishi et al. (2017). They indicate that the younger generations of all five crusts are generally of hydrogenetic origin, as the major manganese mineral is vernadite (∂-MnO_2); no evidence of early-diagenetic buserite was recorded, the Mn/Fe ratio in the samples ranges between 1.1 and 2.3, and they are Co- and Ni-rich (up to 0.3–0.8 wt.%). The oldest age of the younger hydrogenetic generation is around 18 Ma or younger (Nishi et al., 2017), and its growth rate is slow (between 2 and 6 mm/Ma); there is no indication of a significant break or hiatus during their growth throughout the Neogene to present.

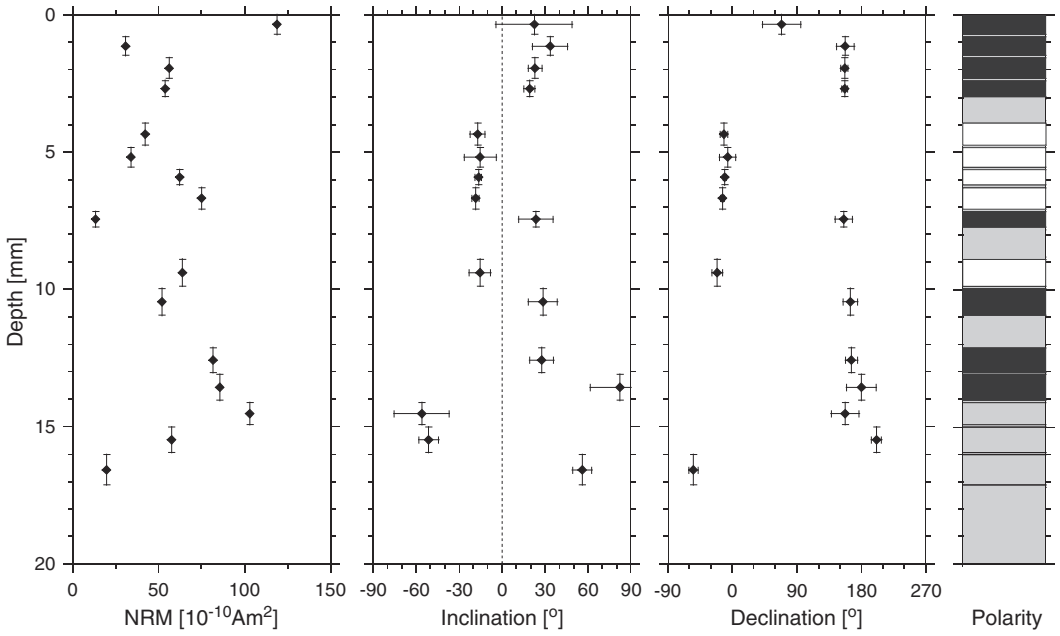

Fig. 4. Depth variations of NRM intensity, ChRM inclination and declination for the Ryukyu sample. An interpreted polarity for each slice is indicated in the rightmost panel: normal polarity is marked in black; reversed polarity in white; unidentified interval in gray (lost interval by cutting or inconclusive polarity). Vertical bars associated with the data points in the left three panels indicate thicknesses of the corresponding slices, whereas horizontal bars with the data points in the middle two panels show 95% confidence limits (α_{95}) of the corresponding slices.

The samples were cut using a diamond blade into rectangular columns, perpendicularly to the wavy layered structure with different cross-sections to locate the structures that are as much parallel as possible to the wavelength (Fig. 2): 18 × 18 mm for the Ryukyu and Ryusei samples; 9 × 6 mm for the Hanzawa sample; 24 × 24 mm for the Takuyo-Daigo sample; and 7 × 7 mm for the Nosappu sample. Then, several reference lines were marked on the side of each column, vertically to the top of the cross-section. The rectangular columns were embedded with a non-magnetic resin and they were further cut with a saw microtome (Leica SP1600) into slices with thicknesses of 0.4–1.1 mm (1.4 mm for two slices from the Takuyo-Daigo sample) parallel to the structures (Fig. 2).

The thickness of each slice was measured with a non-magnetic micrometer. Thickness loss that occurred during the cutting, was calculated by subtracting the total thickness of the slices from the initial height of the column. Following this, an average thickness loss between two adjacent slices was estimated by dividing the total thickness loss by the number of slices cut from each column. A total of 16, 15, 16, 27 and 23 slices were cut from the depths of 0–17.111, 0–14.309, 0–15.812, 0–28.3 and 0–23.186 mm for the Ryukyu, Ryusei, Hanzawa, Takuyo-Daigo and Nosappu samples, respectively. The depth of each slice was measured from the surface of each column and calculated with consideration of the average thickness loss between adjacent two slices. The average thickness loss differed among the columns.

2.2. Paleomagnetic measurements

In order to determine the paleomagnetic directions of the cut slices, stepwise alternating field (AF) demagnetizations and simultaneous remanence measurements were made on natural remanent

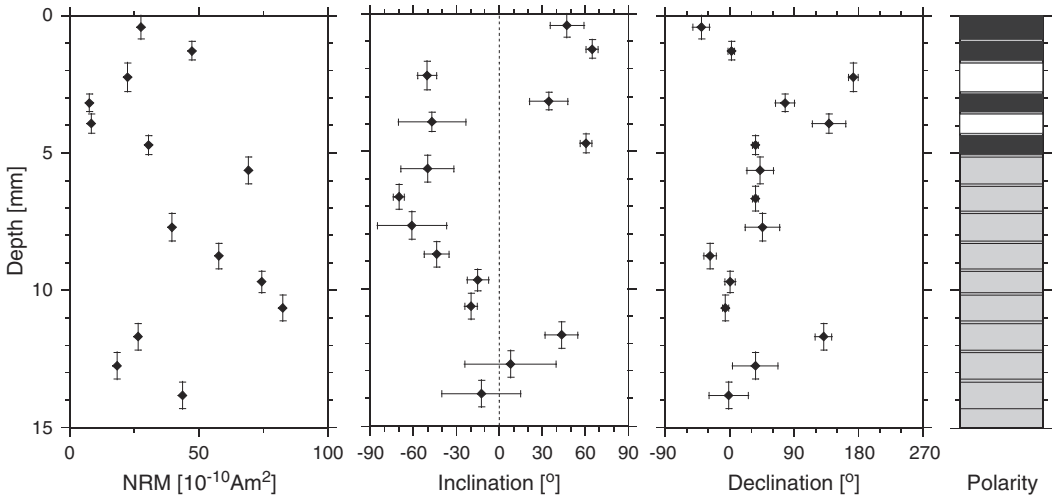

Fig. 5. Depth variations of NRM intensity, ChRM inclination and declination for the Ryusei sample. An interpreted polarity for each slice is indicated in the rightmost panel.

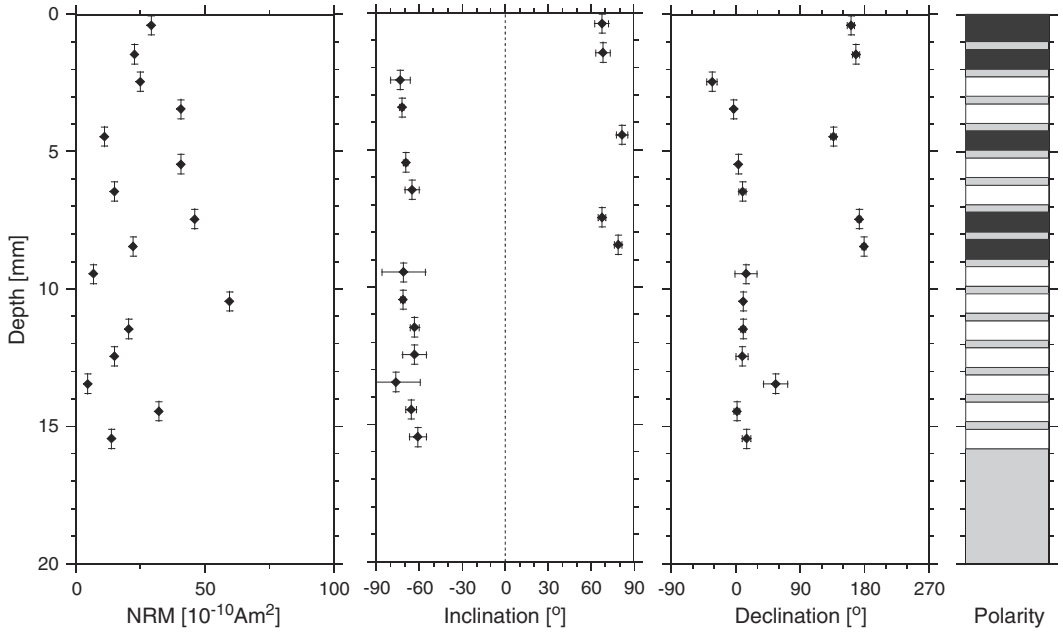

Fig. 6. Depth variations of NRM intensity, ChRM inclination and declination for the Hanzawa sample. An interpreted polarity for each slice is indicated in the rightmost panel.

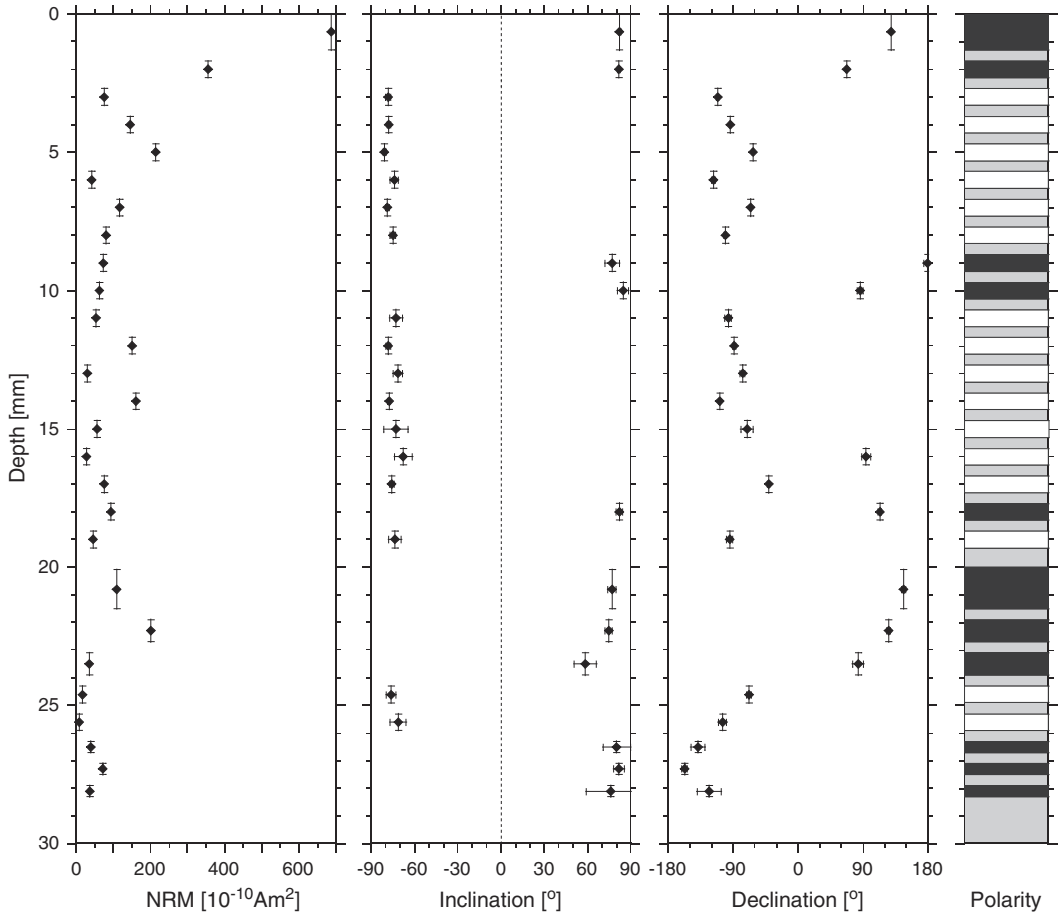

Fig. 7. Depth variations of NRM intensity, ChRM inclination and declination for the Takuyo-Daigo sample. An interpreted polarity for each slice is indicated in the rightmost panel.

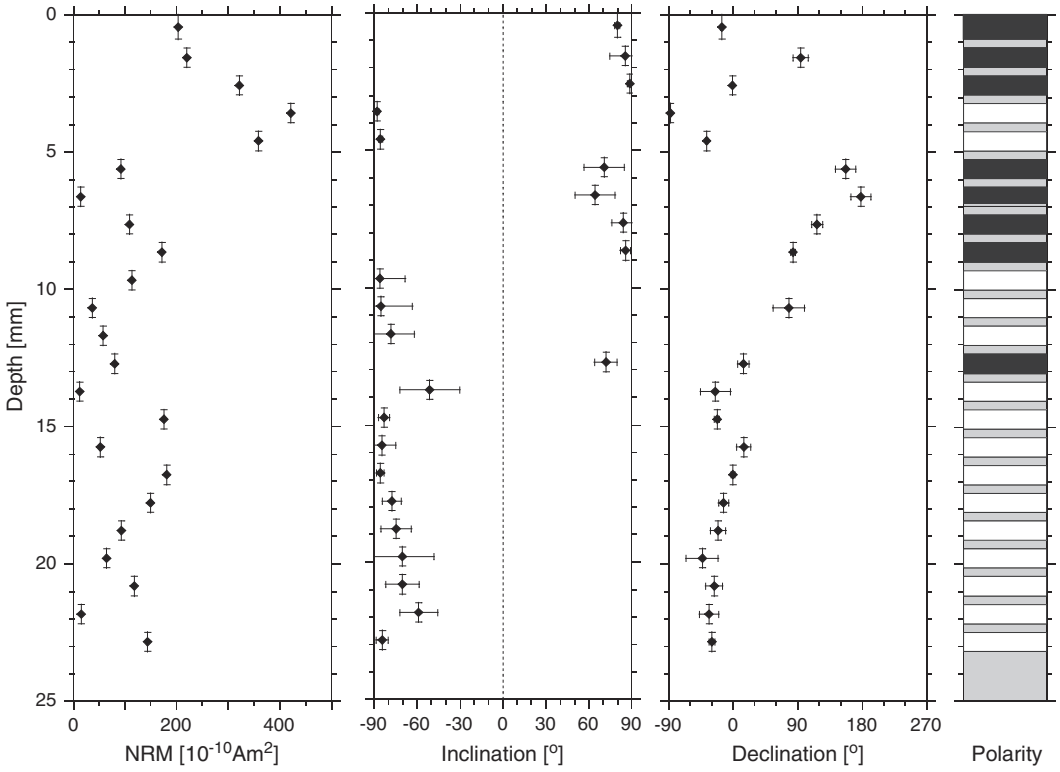

Fig. 8. Depth variations of NRM intensity, ChRM inclination and declination for the Nosappu sample. An interpreted polarity for each slice is indicated in the rightmost panel.

magnetizations (NRMs) of the cut slices. The slices were set in three different ways for demagnetizations and the measurements (Fig. 2):

(1) For the Ryukyu and Ryusei samples, each slice was placed in a plastic cube typically used for paleomagnetic measurements and secured with glass wool.
(2) For the Hanzawa and Nosappu samples, each slice was placed on a lid of the same type of a plastic cube and secured with double-sided tape. The lid was then paired with another lid using a parafilm.
(3) For the Takuyo-Daigo sample, each slice was placed between non-magnetic sponges.

For the Ryukyu, Ryusei, Hanzawa and Nosappu samples, the slices were subjected to tumbling demagnetization at 2–20 mT steps up to 100 mT using an AF demagnetizer (Natsuhara-Giken DEM-95), and their remanences were measured by a DC SQUID magnetometer (2G Enterprises Model 755 — 4.2 cm). For the Takuyo-Daigo sample, a DC SQUID magnetometer with an inline static AF demagnetizer (2G Enterprises Model 760R) was used to demagnetize the slices at 2.5–10 mT steps up to 80 mT and to measure remanences. Utilizing the reference lines, we could set an internally consistent sample coordinate for each column (x, y, and z indicated by orange arrows in Fig. 2). Relative declination was calculated as $D = \tan^{-1}(y/x)$ while inclination as $I = \tan^{-1}(z/\sqrt{x^2+y^2})$. All of these measurements were performed at the paleomagnetic laboratory of the Center for Advanced Marine Core Research (CMCR), Kochi University, Japan. The SQUID magnetometers at CMCR are sensitive enough ($\sim 4 \times 10^{-12}$ A m^2) to provide reliable paleomagnetic data even from a single zircon crystal (e.g. Sato et al., 2015).

3. Results

In most cases, AF demagnetizations at 10–20 mT successfully removed secondary components giving the characteristic remanent magnetizations (ChRMs). Representative vector demagnetization diagrams are shown for each sample in Fig. 3. For example, it is recognized in the Ryukyu sample that the ChRM of the slice from the depth of 2.408–2.971 mm resulted in an inclination of 19.3° and relative declination of 156.8° (Fig. 3(A)) while that of 3.948–4.746 mm resulted in an inclination of −17.1° and relative declination of 348.2° (Fig. 3(B)). They are obviously in antiparallel directions and thus can be considered a paleomagnetic reversal record. The same is true for the other four samples (Fig. 3(C)–(J)). Depth variations of NRM intensity, ChRM inclination and declination for the Ryukyu, Ryusei, Hanzawa, Takuyo-Daigo and Nosappu samples are summarized in Figs. 4, 5, 6, 7 and 8, respectively.

All samples were recovered from the mid-high latitude region in the northern hemisphere, where the Brunhes normal polarity chron has lasted since 0.781 Ma (Gradstein et al., 2012) resulting in positive inclination. The topmost slices cut from the samples commonly yielded positive inclinations and therefore, can be considered records of normal paleomagnetic polarities. The results of negative inclinations are thought to be records of reversed paleomagnetic polarities. Based on this dependence, we assessed the paleomagnetic polarity of each slice (Figs. 4–8).

In the Ryukyu sample, the slices (except for the topmost (0–0.716 mm) and the three lowermost (14.127–17.111 mm)) have positive and negative inclinations accompanied with relative declinations of ~150° and ~−30°, respectively (Fig. 4). These two grouped ChRM directions are antiparallel and thus they seem to faithfully reflect paleomagnetic reversals. The topmost slice yielded the positive inclination of ~20° and the relative declination of ~70°, which is rather close to ~150°. The corresponding paleomagnetic polarity does not seem to be contradicted from a normal polarity. Paleomagnetic polarities of the lowermost three slices are not conclusive, because their ChRM directions (paired values of the inclinations and the relative declinations) are inconsistent with those of the upper slices. Consequently, we obtained a reversal sequence of

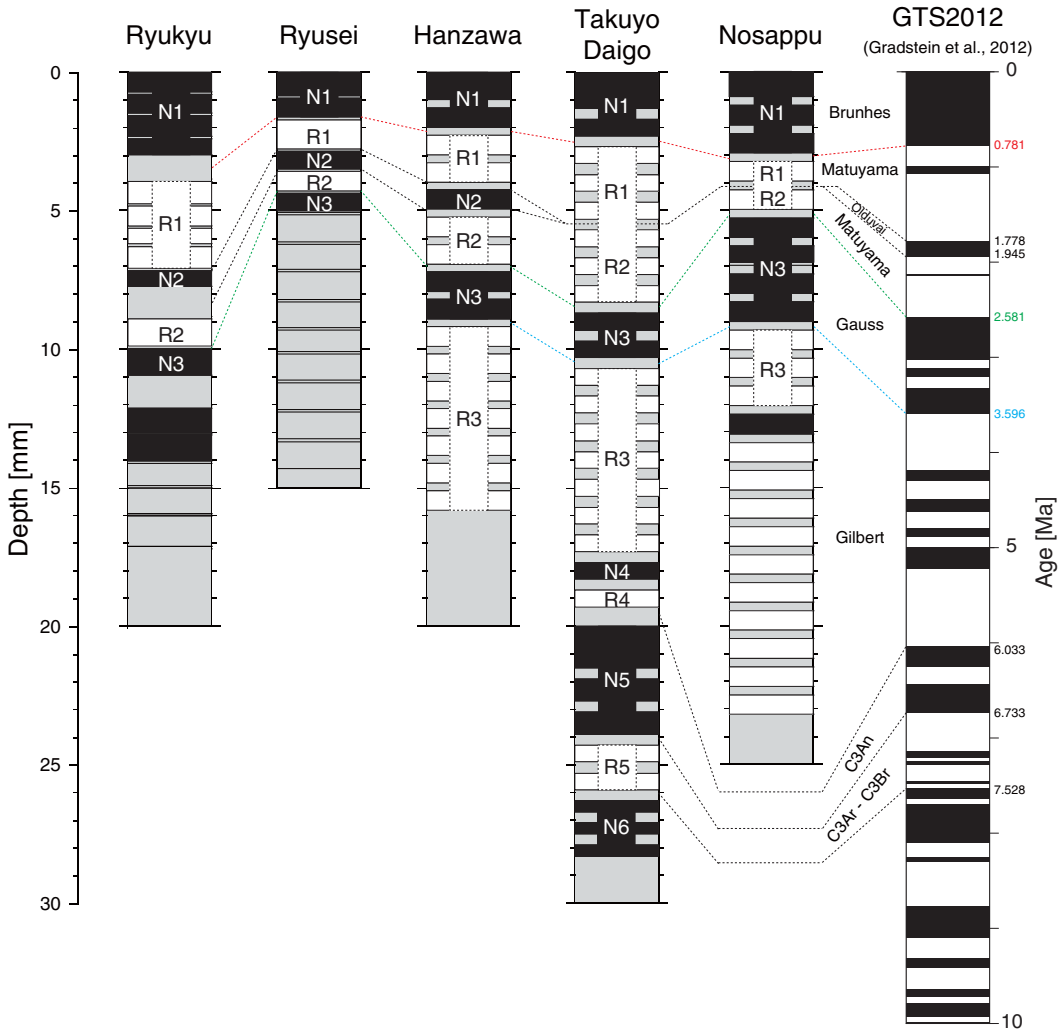

Fig. 9. Comparisons and correlations of the reversal patterns obtained from the five samples. The rightmost panel indicates the geomagnetic polarity time scale based on the chron boundary ages of Geologic Time Scale 2012 (GTS2012; Gradstein et al., 2012). Dotted lines indicate the correlations of the major chron boundaries.

normal–reversed–normal–reversed–normal polarity (N–R–N–R–N) from the surface to the inner part of the sample for the interval of 0–14.039 mm (Fig. 4).

In the Ryusei sample, the six topmost slices (0–5.063 mm) are characterized by two antiparallel ChRM directions: a positive inclination of ~40–60° and relative declination of ~0°; and a negative inclination of ~−50° and relative declination of ~150° (Fig. 5). Thus, they are thought to be the records of paleomagnetic reversals. On the other hand, the ChRM directions of the lower slices (5.153–14.309 mm) are different from these two directions and their paleomagnetic polarities are inconclusive. As a result, a reversal sequence of N–R–N–R from the surface to the inner part of the sample is recognized for the interval of 0–5.063 mm.

The ChRM directions of all the slices from the Hanzawa sample resulted in the two antiparallel directions of (1) a positive inclination of ~70° and relative declination of ~150° and (2) a negative inclination of ~−70° and relative declination of ~0° (Fig. 6). A reversal sequence of N–R–N–R–N–R recognized for the interval of 0–15.812 mm from the surface to the inner part of the sample seems to be robust.

Steep inclinations close to either ~−90° or ~90° are commonly observed for the ChRM directions of the slices from the Takuyo-Daigo and Nosappu samples (Figs. 7 and 8). By definition, declination becomes

Table 1
Relationship between the depths and the chron boundary ages of each sample.

Chron boundary	Correlated depth [mm]					Age [Ma]
	Ryukyu	Ryusei	Hanzawa	Takuyo-Daigo	Nosappu	Gradstein et al. (2012)
Brunhes/Matuyama	3.46 ± 0.49	1.67 ± 0.05	2.13 ± 0.14	2.50 ± 0.20	3.08 ± 0.16	0.781
Upper-Matuyama/Olduvai	7.13 ± 0.04	2.82 ± 0.05	4.11 ± 0.14			1.778
Olduvai/lower-Matuyama	8.32 ± 0.59	3.54 ± 0.05	5.09 ± 0.14			1.945
Matuyama/Gauss	9.93 ± 0.04	4.33 ± 0.05	7.07 ± 0.14	8.50 ± 0.20	5.11 ± 0.16	2.581
Gauss/Gilbert			9.04 ± 0.14	10.50 ± 0.20	9.16 ± 0.16	3.596
Gilbert/C3An				19.65 ± 0.35		6.033
C3An/C3Ar–C3Br				24.10 ± 0.20		6.733
C3Ar–C3Br/C4n				26.10 ± 0.20		7.528

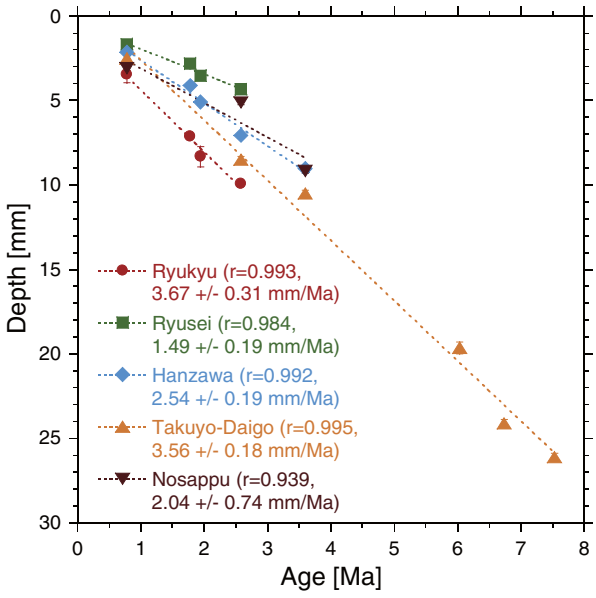

Fig. 10. The relationship between the depth and the chron boundary age of the five samples based on the magnetostratigraphic correlations shown in Fig. 9 and Table 1. Dashed lines indicate results of linear regressions for the relationships.

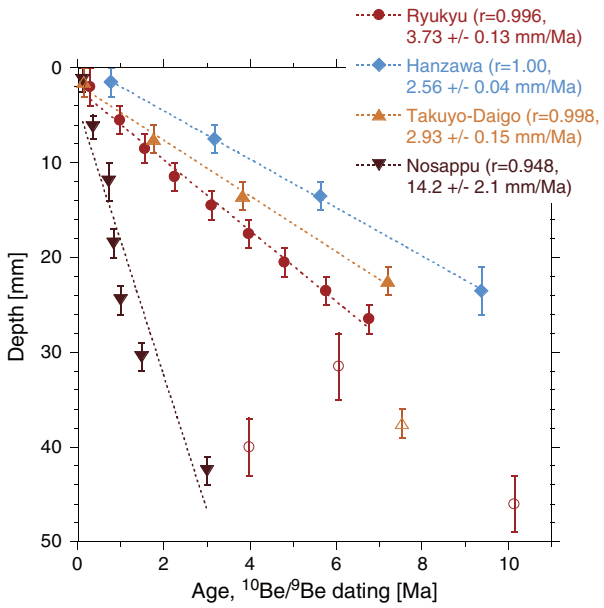

Fig. 11. Relationships between depth and age of the Ryukyu, Hanzawa, Takuyo-Daigo and Nosappu samples estimated with $^{10}Be/^{9}Be$ method. Dashed lines indicate results of linear regressions for the relationships (data points marked with open symbols are not included).

ambiguous when inclination is approaching ±90°, and it does not seem to be appropriate to take declination into account for identification of paleomagnetic polarities. Based on the obtained inclinations, a reversal sequence of N–R–N–R–N–R–N–R–N (N–R–N–R–N–R) can be established from the surface to the inner part of the sample for the interval of 0–28.3 (0–23.186) mm for the Takuyo-Daigo (Nosappu) sample.

4. Discussion

The reversal sequences seem to show a consistent reversal pattern from the surface to the inner part for all five samples: N1–R1–N2–R2–N3 (Fig. 9). An older polarity interval than N3, interval R3, was recognized in three samples (Hanzawa, Takuyo-Daigo and Nosappu). Even though the interval N2 seems to be missing in two samples (Takuyo-Daigo and Nosappu), ferromanganese crusts in the northwest Pacific commonly record paleomagnetic reversals and reversal patterns deduced from the crusts can be used for ocean-scale correlations.

During the last few million years, four well-known major polarity chrons were noted: Brunhes (normal polarity, 0–0.781 Ma), Matuyama (reversed, 0.781–2.581 Ma), Gauss (normal, 2.581–3.596 Ma) and Gilbert (reversed, 3.596–6.033 Ma); and a major subchron of Olduvai (normal, 1.778–1.945 Ma) during the Matuyama chron. Assuming no hiatuses, the polarity intervals N1, R1, N2, R2, N3 and R3 seem to be correlated with Brunhes, upper Matuyama, Olduvai, lower Matuyama, Gauss and Gilbert chrons, respectively (Fig. 9). Another reversal sequence, N4–R4–N5–R5–N6, is recognized for the Takuyo-Daigo sample, and these may also be correlated to chrons (Fig. 9). These correlations yield depths corresponding with each chron boundary for the five samples as indicated by dotted lines in Fig. 9, and the relationships between the depths and the chron boundary ages are summarized in Table 1. Note that chron boundary ages are referred to the Geologic Time Scale 2012 (GTS2012) by Gradstein et al. (2012).

The relationship between depths and chron boundary ages for each sample (Fig. 9 and Table 1) is illustrated in Fig. 10. Linear regressions applied to the relationships resulted in high correlation coefficients (r): 0.993, 0.984, 0.992 and 0.995 for Ryukyu, Ryusei, Hanzawa and Takuyo-Daigo samples, respectively. It is implied that the four crusts grew continuously with rates of 3.67, 1.49, 2.54 and 3.56 mm/Ma, at least for the surficial layers of ~4–26 mm (Fig. 10 and Table 2). On the other hand, the Nosappu sample might have moved and/or rotated during its growth resulting in a non-constant growth and a relatively low correlation coefficient of 0.939; it is the only sample taken by a dredge and therefore its orientation is not known.

We performed $^{10}Be/^{9}Be$ dating on the Ryukyu, Hanzawa, Takuyo-Daigo and Nosappu samples with Accelerated Mass Spectroscopy at the GNS Science, Lower Hutt, New Zealand, using the methods described by Graham et al. (2004) and Usui et al. (2007). A ^{10}Be half-life of 1.387 ± 0.012 myr (Chmeleff et al., 2010) and a $^{10}Be/^{9}Be$ initial value of $1.29 \pm 0.05 \times 10^{-7}$ were used (Oda et al., 2011). The relationships between depths and $^{10}Be/^{9}Be$ ages suggest nearly constant growth rates of 3.73, 2.56 and 2.93 mm/Ma with high correlation coefficients ($r \geq 0.996$; $n = 9$, 4 and 4) of the linear regressions for the Ryukyu, Hanzawa and Takuyo-Daigo samples, respectively, except for outlier data points ($n = 3$ for Ryukyu and $n = 1$ for Takuyo-Daigo) (Fig. 11). For the Nosappu sample, the linear regression also implies a constant growth rate of 14.2 mm/Ma with a lower correlation coefficient ($r = 0.948$; $n = 7$). It is apparent that the estimated growth rates for the Ryukyu, Hanzawa and Takuyo-Daigo samples are consistent with the magnetostratigraphic and the $^{10}Be/^{9}Be$ dating methods at the 2σ (standard deviation) level (Table 2).

Table 2
Growth rates estimated with the magnetostratigraphic and $^{10}Be/^{9}Be$ methods. The units are mm/Ma, and the values are shown with 1σ (standard deviation).

	Ryukyu	Ryusei	Hanzawa	Takuyo-Daigo	Nosappu
Magnetostratigraphic method	3.67 ± 0.31	1.49 ± 0.19	2.54 ± 0.19	3.56 ± 0.18	2.04 ± 0.74
$^{10}Be/^{9}Be$ method	3.73 ± 0.13		2.56 ± 0.04	2.93 ± 0.15	14.2 ± 2.1

Although the magnetostratigraphic method is demonstrated to be successful, a more novel technique to obtain ultrafine-scale magnetostratigraphy is necessary, especially for geologically younger samples. It is known that the rate of paleomagnetic reversals has varied during the last 300 Ma (Merrill et al., 1998; Olson and Amit, 2015), and the rate of 0–20 Ma is high (~4–5 times/Ma). For example, if the growth rate was ~2 mm/Ma, a chron series (polarity) during 0–20 Ma would be detected only by using a sample interval of 0.4–0.5 mm in a ferromanganese crust. It is difficult to prepare a cut slice with such a thin interval, and a similar interval tends to be lost with every cutting even if the preparation was successful. Actually, in the present study, the polarity interval N2 that is correlated to the Olduvai normal subchron (1.778–1.945 Ma) is not found in the Takuyo-Daigo and Nosappu samples, but in the Ryukyu, Ryusei and Hanzawa samples (Fig. 9). Based on the estimated growth rates by the magnetostratigraphic method (Table 2), the expected thicknesses for the Olduvai subchron in the five samples are 0.25–0.61 mm. It seems fortuitous that this subchron was not lost during the cutting, but preserved in a cut slice. Oda et al. (2011) introduced a magnetostratigraphy with ~85 μm spatial resolution for a marine ferromanganese crust using SQUID microscopy, and this kind of approach is expected to allow more exact and accurate growth-rate estimates of ferromanganese crusts.

5. Conclusions

Thin slices with thicknesses of 0.5–1.0 mm cut from ferromanganese crusts recovered from five locations in the northwest Pacific (Ryukyu, Ryusei, Hanzawa, Takuyo-Daigo and Nosappu) gave consistent reversal patterns. Ferromanganese crusts in the northwest Pacific are thus thought to record common paleomagnetic reversals with their reversal patterns usable for ocean-scale correlations. Except for the Nosappu sample, the magnetostratigraphic method indicates constant growth rates for the four samples of 1.49, 2.54, 3.56 and 3.67 mm/Ma, three of which are consistent with growth rates determined using $^{10}Be/^{9}Be$ dating at the 2σ (standard deviation) level.

Acknowledgements

YY and AU were partially supported by a cross-ministerial strategic innovation promotion program (SIP) funded by the Japanese government (Geosciences on Mineral Diversity of Marine Manganese Deposits, Next-generation Technology for Ocean Resources Exploration). HO was also partially supported by JSPS Grant-in-Aid for Scientific Research (A) Funding Nos. 25247082 and 25247073.

References

Chan, L.S., Chu, C.L., Ku, T.L., 1985. Magnetic stratigraphy observed in ferromanganese crust. R. Astron. Soc. Geophys. J. 80, 715–723.

Chmeleff, J., von Blanckenburg, F., Kossert, K., Jakob, D., 2010. Determination of the ^{10}Be half-life by multicollector ICP-MS and liquid scintillation counting. Nucl. Instrum. Methods Phys. Res., Sect. B 268, 192–199. http://dx.doi.org/10.1016/j.nimb.2009.09.012.

Gradstein, F.M., Ogg, J.G., Schmitz, M.D., Ogg, G.M. (Eds.), 2012. The Geological Time Scale. Elsevier, Amsterdam, p. 2012.

Graham, I.J., Carter, R.M., Ditchburn, R.G., Zondervan, A., 2004. Chronostratigraphy of ODP 181, Site 1121 sediment core (Southwest Pacific Ocean), using $^{10}Be/^{9}Be$ dating of entrapped ferromanganese nodules. Mar. Geol. 205, 227–247.

Joshima, M., Usui, A., 1998. Magnetostratigraphy of hydrogenetic manganese crusts from northwestern Pacific seamounts. Mar. Geol. 146, 53–62. http://dx.doi.org/10.1016/S0025-3227(97)00131-X.

Lee, T.G., Lee, K., Hein, J.R., Moon, J.W., 2009. Geophysical investigation of seamounts near the Ogasawara Fracture Zone, western Pacific. Earth Planets Space 61, 319–331.

Linkova, T.I., Ivanov, Y.Y., 1993. Magnetic stratigraphy in ferromanganese crusts from Central Pacific. Geol. Pac. Ocean 9, 187–197.

Merrill, R.T., McElhinny, M.W., McFadden, P.L., 1998. The Magnetic Field of the Earth — Paleomagnetism, the Core, and the Deep Mantle. Academic Press, California, p. 531.

Nishi, K., Usui, A., Nakasato, Y., Yasuda, H., 2017. Formation age of the dual structure and environmental change recorded in hydrogenetic ferromanganese crusts from the Northwest and Central Pacific seamounts. Ore Geol. Rev. 87, 62–70.

Oda, H., Usui, A., Miyagi, I., Joshima, M., Weiss, B.P., Shantz, C., Fong, L.E., McBride, K.K., Harder, R., Baudenbacher, F.J., 2011. Ultrafine-scale magnetostratigraphy of marine ferromanganese crust. Geology 39, 227–230. http://dx.doi.org/10.1130/G31610.1.

Olson, P., Amit, H., 2015. Mantle superplumes induce geomagnetic superchrons. Front. Earth Sci. 3, 38.

Sato, M., Yamamoto, S., Yamamoto, Y., Okada, Y., Ohno, M., Tsunakawa, H., Maruyama, S., 2015. Rock-magnetic properties of single zircon crystals sampled from the Tanzawa tonalitic pluton, central Japan. Earth Planets Space 67, 150. http://dx.doi.org/10.1186/s40623-015-0317-9.

Usui, A., Graham, I.J., Ditchburn, R.G., Zondervan, A., Shibasaki, H., Hishida, H., 2007. Growth history and formation environments of ferromanganese deposits on the Philippine Sea Plate, northwest Pacific Ocean. Island Arc 16, 420–430. http://dx.doi.org/10.1111/j.1440-1738.2007.00592.x.

Usui, A., Nishi, K., Sato, H., Nakasato, Y., Thornton, B., Kashiwabara, T., Tokumaru, A., Sakaguchi, A., Yamaoka, K., Kato, S., Nitahara, S., Suzuki, K., Iijima, K., Urabe, T., 2017. Continuous growth of hydrogenetic ferromanganese crusts since 17 Myr ago on Takuyo-Daigo Seamount, NWPacific, at water depths of 800–5500 m. Ore Geol. Rev. 87, 71–87.